Anesthetic Block of Pain-related Cortical Activity in Patients with Peripheral Nerve Injury Measured by Magnetoencephalography

Peter J. Theuvenet, M.D.,* Jan C. de Munck, Ph.D.,† Maria J. Peters, Ph.D.,‡ Jan M. van Ree, Ph.D.,§ Fernando L. Lopes da Silva, Ph.D.,‖ Andrew C. N. Chen, Ph.D.#

ABSTRACT

Background: This study examined whether chronic neuropathic pain, modulated by a local anesthetic block, is associated with cortical magnetic field changes.

Methods: In a group of 20 patients with pain caused by unilateral traumatic peripheral nerve injury, a local block with lidocaine 1% was administered and the cortical effects were measured and compared with a control group. The global field power (GFP), describing distribution of cortical activation after median and ulnar nerve stimulation, was plotted and calculated. The effects on the affected hemisphere and the unaffected hemisphere (UH) before and after a block of the injured nerve were statistically evaluated.

Results: Major differences based on the GFP curves, at a component between 50 ms - 90 ms (M70), were found in patients: in the affected hemisphere the M70 GFP peak values were statistically significantly larger in comparison with the UH, and the GFP curves differed morphologically. Interestingly, the mean UH responses were reduced in comparison with the control group, a finding suggesting that the UH is also part of the cortical changes. At M70, the GFP curves and values in the affected hemisphere were modulated by a local block of the median or the ulnar nerve. The most likely location of cortical adaptation is in the primary somatosensory cortex.

Conclusions: Cortical activation is enhanced in the affected hemisphere compared with the UH and is modulated by a local block. The UH in neuropathic pain changes as well. Evoked fields may offer an opportunity to monitor the effectiveness of treatments of neuropathic pain in humans.

What We Already Know about This Topic

- Peripheral nerve injury leading to pain can cause neuroplasticity in the brain, although the extent and acute reversibility of these changes are relatively unexplored

What This Article Tells Us That Is New

- Magnetoencephalography in 20 patients with unilateral peripheral nerve injury and pain compared to control demonstrated bilateral cortical changes which were acutely reversed by peripheral nerve block of the affected extremity

TRAUMATIC peripheral nerve injury (PNI) may produce a variety of symptoms including neuropathic pain, autonomic dysfunction, and disability.[1–3] Functionally, neuropathic pain may result from abnormal peripheral inputs and/or abnormal central processing.[4–8] The continuous volleys of ectopic afferent inputs produce central adaptive changes.[9–16] Neurophysiologic parameters that characterize these cortical changes range from peak latency differences to cortical map reorganization.[17–20] Anatomic changes caused by sprouting and growth into the deafferentiated area were found in animals after sensory loss of a forelimb.[21,22] In humans, electroencephalography studies showed functional changes in cortical evoked responses in amputees[19,23–25] after nerve injuries[10,26,27] and after stroke using magnetoencephalography.[28] After nerve injury in humans, cortical changes whereby recruitment from neighboring cortical areas occurred, also were reported.[2,15,29–31]

Supplemental digital content is available for this article. Direct URL citations appear in the printed text and are available in both the HTML and PDF versions of this article. Links to the digital files are provided in the HTML text of this article on the Journal's Web site (www.anesthesiology.org).

* Specialist, Project Coordinator, Department of Anesthesiology-Pain Clinic, Medical Centre Alkmaar, Alkmaar, The Netherlands. † Assistant Professor, Department of Physics and Medical Technology, VU University Hospital, Amsterdam, The Netherlands. ‡ Professor Emeritus, Twente Technical University, Low Temperature Division, Enschede, The Netherlands. § Professor, Rudolf Magnus Institute of Neuroscience, Utrecht, The Netherlands. ‖ Professor Emeritus, Swammerdam Institute for Life Sciences, Center of NeuroSciences, Amsterdam, The Netherlands. # Professor, Centre for Higher Brain Functions, Capital University, Beijing, China.

Received from the Medical Centre Alkmaar, Pain Clinic, Alkmaar, The Netherlands. Submitted for publication September 6, 2010. Accepted for publication March 23, 2011. Supported by a grant (RA20040601) from Medtronic Europe Sàrl, Tolochenaz, Switzerland. This is a basic scientific study and fully unrelated to commercial aims. No single patient received an implantable device during the study (spinal cord stimulator or implantable pump system) or has there been any unwanted obligation in this respect. There is also no indirect interest by a third party.

Address correspondence to Dr. Theuvenet: Oranjelaan 61, 1815 JR Alkmaar, The Netherlands. p.theuvenet@tiscali.nl. Information on purchasing reprints may be found at www.anesthesiology.org or on the masthead page at the beginning of this issue. ANESTHESIOLOGY's articles are made freely accessible to all readers, for personal use only, 6 months from the cover date of the issue.

 Anesthesiology 2011; 115:375–86

Nonetheless, central adaptations and sensitization in humans are difficult to demonstrate, and pain modulation at the cortical level is not well established.[32–34]

In this study, we hypothesized that the volley of impaired afferent information in the PNI group, as soon as it was interrupted by a local anesthetic block, would result in detectable cortical changes. Advances in magnetoencephalography, characterized by its accurate detection of fissural generators and undisturbed by reference activity, provides a better temporal resolution of the functional brain changes than functional magnetic resonance imaging (MRI). The aim of this study was to explore the cortical effects of local anesthesia at the site of the nerve injury and to test the reversibility of the functional cortical changes using magnetoencephalography. We compared the characteristics of the evoked cortical fields after electrical stimulation of the median and/or ulnar nerve in two groups: a group of healthy subjects and a group of patients with traumatic PNI in one upper extremity and the same patient group remeasured after local anesthesia in the pain-free condition.

Materials and Methods

The study was approved by the Medical Ethical Committee Alkmaar (NH04-196) and the VU Hospital Amsterdam. All healthy subjects and patients were adequately informed and gave their written consent. Twenty healthy subjects (13 males and 7 females, age range 27–48 yr, mean 34.1, SD ± 6.1 yr), all Caucasian and right-handed) were recruited from two hospital staffs. Twenty patients with a traumatic nerve injury and continuous pain were studied. Table 1 presents demographic data of the PNI group. Although variation of the nerve injuries is observed, all were in pain.

The group consisted of 5 male and 15 female right-handed patients; age was between 22 and 69 yr (mean 48.3 and SD ± 14.7 yr). In all patients, neuropathic pain had been present between 1–25 yr (mean 5.4 SD ± 6.5 yr). In 13 of 20 patients, traumatic nerve injury was assessed during microsurgical repair, secondary neurolysis after a carpal tunnel syndrome (N = 2), after surgery for de Quervain syndrome and neuroma forming (N = 3) or after a metacarpal fracture (N = 2). Neuroanatomic damage varied from full nerve transection to digital nerve injury. In five patients after major nerve injury (A-1, A-3, A-4, A-6, A-11) partial paralysis or paresis was found; patient A3 also suffered from spasms. Mechanical allodynia was present in all patients, with change in severity prompted by the level of activity. Other sensory symptoms included hyperalgesia, hypoesthesia, and paraesthesia. All patients complained of a cold hand, particularly during severe pain. Trophic changes included hyperhidrosis. The diagnosis of complex regional pain syndrome is based on signs and symptoms.[35,36] At the time of the measurements in 5 of 20 patients, this syndrome was diagnosed. Patient A-7, who only had a radial branch injury after surgery for de Quervain syndrome, suffered from pain for 22 yr. Considerable edema, dystonia, and loss of function were intermittent symptoms. The verbal rating score before the measurements ranged from 4 to 9 (mean 7.0, SD ± 1.0); after the local block each patient had to be pain free. At the time of admission to the pain clinic, analgesics (nonopioids and opioids) and antiepileptic agents all had been used without good results. Patients randomly used different medications such as paracetamol and nonsteroidal antiinflammatory drugs and opioids such as tramadol or morphine. Three to 7 days before the measurements, patients were free of pain medication. No neurologic diseases were present and no medication was used that might bias cortical results (*i.e.*, antiepileptic agents).

Measurements

In the subject group, the four possible stimulation sites of both hands received a number, the left median nerve a "1" and the left ulnar a "2," for the right side "3" and "4" respectively. Stimulation order of the median or ulnar nerve was performed in a randomized way (*i.e.*, 4, 2, 1, 3 for subject HC-04) with a bipolar electrode at the wrist and the cathode placed proximally.[37] For patients, to avoid inducing additional pain, we stimulated the nerves parallel to the injured nerves, *e.g.*, after median/radial nerve injury the ulnar evoked responses were studied. Stimulation of the nerve parallel to the injured painful nerve is supported by experiments in squirrel monkeys and in human subjects where dominance of the adjacent intact nerve emerged cortically.[38–40] Subjects and patients were measured in the supine position under identical conditions, for a duration of approximately 45 min with the head well positioned in the helmet. Foam rubber and the position of the bed close to the helmet stabilized the head in the helmet without much space left to move, which might alter the position. A resting period between stimulation sessions of 5–10 min was ensured. An electrical nerve stimulator (Grass, model S48, Pegasus Scientific Inc., Rockville, MD) and photoelectric stimulus isolation unit (Grass, model SIU7) was used. The stimulation current was pulsed at a repetition rate of 2 Hz with a pulse duration of 0.2 ms. In 10 of 20 patients, median nerve stimulation and ulnar nerve stimulation were performed. Patients were measured three times: first, on the unaffected side, and then on the affected side before and after the administration of a local anesthetic block (2 ml lidocaine 1%) subcutaneously at the painful site (affected hemisphere [AH] block). Full pain alleviation was achieved in 16 of 20 patients after 15 min. In four patients, a fourth measurement was performed because full pain alleviation required a second block. A distinction was made between the AH and UH; the AH and UH correspond to the contralateral side of affected and unaffected extremity, respectively. Stimulus intensity threshold reached a 1.5-fold motor twitching level.[41] Five hundred stimuli were recorded from each nerve; after 100 stimuli the position of the head to the helmet was electronically reassessed for accuracy. The peristimulus interval was 50–100 ms pretrigger and 400 ms posttrigger. During measurements, subjects and patients were asked to ignore the stimuli and refrain from blinking as much as possible, to keep eyes open, and fixate on a point on

Table 1. Demographic Data of PNI Patients

Patient	Age	Sex	Injured Nerve	Etiology and Operation	Number*	Onset of Pain	Pain Duration (yr)
A-1	35	F	Median nerve	Glass wound wrist, subtotal transection	3	Immediately after trauma	4
A-2	43	M	Radial nerve	Sharp trauma, wrist, secondary entrapment correction	3	Immediately after suture	3
A-3	47	M	Median nerve	Glass wound, total transection, median repair	1	2–3 months after injury	7
A-4	54	M	Median nerve	Glass wound, primary suture, neuroma removal	2	Few weeks later	9
A-5	29	F	Radial nerve	Ganglion operation at wrist three times, radial nerve neuroma	1	Few weeks later	10
A-6	30	F	Median nerve	Glass wound, 50% transection	2	1 month later	1
A-7	63	F	Radial nerve	de Quervain, wrist, nerve branch transection, neurolysis	4	Immediately after operation	22
A-8	22	F	Ulnar nerve	Blunt trauma, ulnar transposition right	2	Before first operation	3
A-9	49	M	Radial nerve	Sharp trauma: neurolysis right hand	2	2 months	3
A-10	61	F	Radial nerve	de Quervain, wrist, pain and sensory loss	1	Immediately after operation	1
A-11	55	M	Ulnar nerve	Neurinoma excision above elbow, infection wound	3	Before first operation	4
A-12	63	F	Rradial nerve	de Quervain, wrist, radial nerve branch entrapment	5	Immediately after operation	25
A-13	69	F	Digit II nerve	Neuroma excision twice	2	Immediately after operation	2
A-14	67	F	Digit V nerve	Metacarpal fracture, neuroma forming digital nerve	2	Immediately after operation	3
A-15	53	F	Median nerve	CTS operation	1	Before first operation	4
A-16	60	F	Digit II nerve	Metacarpal fracture, sensory loss, and pain	0	Within weeks	2
A-17	48	F	Median nerve	CTS operation	1	Before first operation	4
A-18	49	F	Digit II nerve	Digital nerve, local exploration and infection	1	Before first operation	2
A-19	36	F	Ulnar nerve	Knife wound at wrist	2	Immediately after operation	4
A-20	25	F	Digit II nerve	Knife wound at butchery	1	Within weeks	2

Demographic data of all 20 PNI patients. Age, sex, injured nerve, and etiology are presented. Onset of pain after nerve injury and pain duration in years.

* Number of operations after trauma.

CTS = carpal tunnel syndrome; PNI = peripheral nerve injury.

the ceiling. Stimulations were tolerable for both groups during all measurements. Two patients were unable to maintain their position and were left out of the study.

Magnetoencephalographic–MRI Recordings

A 151-channel whole-head magnetoencephalography system (VSM-CTF, Port Coquitlam, British Columbia, Canada) was used and measurements were performed in a three-layer magnetically shielded room (Vacuum Schmeltze GmbH, Hanau, Germany). The x, y, and z coordinate system, common to each individual magnetoencephalography and MRI, was based on three anatomic landmarks and fixed to nasion, left and right preauricular points. Using the positions of these fiducials, a head-centered coordinate frame was defined. The (+) axis was directed to the nose, the (+) y-axis to the left ear and the (+) axis to the vertex. Magnetoencephalographic signals were sampled at 1,250 Hz, triggered by the synchronization pulse of the electric stimulator. Online, filters were

set at direct current for high pass and at 400 Hz (fourth order Butterworth filter - IMST GmbH, Kamp-Lintfort, Germany) for antialiasing low pass. Offline, the magnetoencephalographic data were screened for artifacts, averaged, and direct current-corrected using the pretrigger interval to determine the recording offset. Furthermore, ± averages were calculated to obtain noise level estimates. The raw data were visually inspected after data acquisition. Trials showing clear artifacts caused by eye blinks or by muscle activity, *e.g.*, due to swallowing, were removed from the dataset. MRI registration was performed with a 1.5-T 3-day MRI (Siemens Sonata, Erlangen, Germany).

Data Management and Statistical Analysis

This study was designed as an explorative study for the parameters that describe the cortical evoked differences between healthy subjects and PNI patients. Because no previous experimental and quantitative results as to the magnitude of the expected effects were available, a formal calculation of a prespecified power was not possible. Absence of an *a priori* power analysis indicates that negative statistical results have to be interpreted with caution because an existing difference may not be detected. Based on the low availability of PNI patients with continuing pain, groups of 20 subjects and patients were selected. Experimental design consisted in all cases of simple two-group comparisons. Statistical tests used were the independent groups Student *t* test (or its nonparametric equivalent the Mann–Whitney U test where appropriate) for between-groups comparisons, and the paired Student *t* test (or its nonparametric equivalent the Wilcoxon signed rank test where appropriate) for within-groups comparisons. A *P* value less than 0.05 was considered as a statistically significant rejection of the null-hypothesis specified with two-tailed alternative hypotheses. Effect sizes and *P* values are reported wherever relevant magnitudes of effects existed. Whereby:

$$\text{Effect Size (ES)} = \frac{\text{mean experimental group} - \text{mean control group}}{\text{standard deviation control group}}$$

The effect size (ES)[42,43] is a numeric way of expressing the strength or magnitude of a reported relationship, be it causal or not. An ES near 0.0 means that, on average, the experimental group and control group performed the same; a negative ES, on average, means that the control group performed better. A positive ES means that the experimental group performed better than the control group. The more effective the intervention the higher the positive ES value. Statistical analysis was performed using SigmaStat 3.5v software (Systat Software, Inc. Point Richmond, CA). Control for multiple testing was deemed unnecessary because in this explorative study no common hypothesis or theory covering two or more individual statistical tests was present. Control for the familywise error rate is important only when a conclusion based on several statistical tests is falsified, if at most one of the underlying tests is negative.[44] Given the clinical significance of our results and the likelihood of an increase of type II errors, control for the family wise error rate, *i.e.*, a Bonferroni correction, was not performed.[45,46] Only contralateral hemispherical activity was analyzed in this study for comparison of the subject and patient groups. A Compressed Waveform Profile (CWP), the butterfly-like display of the superimposed evoked responses of all sensors of all subjects and patients, was made. Of each subject and patient, the global field power (GFP) curves and peak values after nerve stimulation of each hand were plotted and calculated to identify power differences and changes after the blocks. The GFP (in femtoTesla^2) was computed for each individual as the sum of squares over all channels, divided by the number of channels (N = 151). For magnetoencephalography, the GFP is a measure of the variability of the magnetic field energy distribution and reflects neuronal activity.[47–49] Together with the CWPs, peak stages and peak latencies were identified. Three stages were defined: an early (less than 50 ms), middle (50 ms-90 ms), and a late stage (90 ms-400 ms). Peaks in the poststimulus 400-ms time window, with clear dipolar somatosensory-evoked field activity, were selected as the cortical areas of interest for analysis. A peak was identified by visual inspection and defined by an amplification factor (= poststimulus amplitude/the prestimulus root mean square value as an indication of noise) >3. Peaks in each of these stages are presented as, *i.e.*, M20 for the peak around 20 ms, *etc*. Three-dimensional cortical maps were made for all subjects (left hemisphere and right hemisphere) and patients (UH, AH, and AH block) at different latencies. VSM - CTF software[50] was used to model the single equivalent current dipole (ECD) sources and Advanced Neuro Technology software (ANT A/S, Enschede, The Netherlands) for graphic display. The conventional single moving dipole analysis[51] was used for magnetoencephalographic data evaluation and based on individual MRIs.

Results

Stimulus Intensities. In the subject and patient group and between the two groups, no significant threshold differences were found between the left and right hand for all stimulated nerves and for all conditions ($P > 0.05$ and ES values). For somatosensory-evoked field peak stages,the incidences and latencies of the peaks in the early, middle, and late stages for subjects and patients were assessed. The number of peaks demonstrated high consistency for both groups. Between the subject and patient groups, at M20, M30, and M70, no consistent significant latency differences were found that indicated facilitation of nerve transmission for patients (see Supplemental Digital Content 1, http://links.lww.com/ALN/A748, listing the number of peaks and peak latencies for both groups).

Characteristics of the CWP

The CWP morphologies of all subjects and patients, after median and ulnar nerve stimulation, demonstrated large

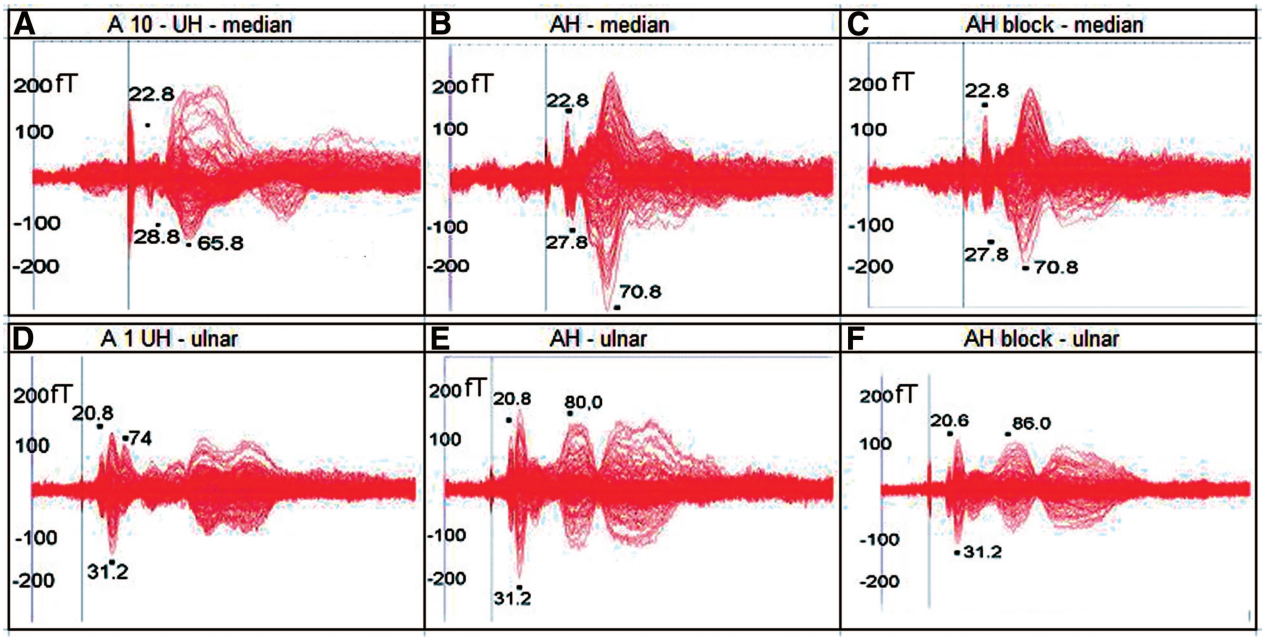

Fig. 1. CWPs after median (*A–C*) and ulnar nerve (*D–F*) stimulation are presented of the UH, AH, and AH block of two patients (A-10 and A-1). The AH block depicts the cortical evoked effects of the block on the affected hemisphere, in the pain-free state. Numbers at various peaks depict the latencies, in *A* the first peak is at 22.8 MS, *etc*. On the y-axis, the amplitude in femtoTesla (fT) is depicted on the x-axis, time in milliseconds (0–400 MS). AH = affected hemisphere; AH-block = affected hemisphere after a local block; CWPs = Compressed waveform profiles; UH = unaffected hemisphere.

interindividual variation but fewer intraindividual hemispherical differences. The CWPs of two patients are presented in figure 1, each from the median and ulnar group, and displayed different profiles. In patient A-10 (fig. 1A–C), the CWPs after median nerve stimulation of both hands before and after the anesthetic block of the affected hand are presented. After ulnar stimulation in patient A-1 (fig. 1D–F) a similar configuration was observed.

The effect of the anesthetic block on the amplitude (reduction) once the patient was pain free, is observed in the middle stage in both patients (fig. 1C and fig. 1F).

GFP Morphology

For the subject and patient groups, GFP plots were made of the 400-ms poststimulus time window. Results are depicted in figure 2. For subjects, LH Med denotes the mean

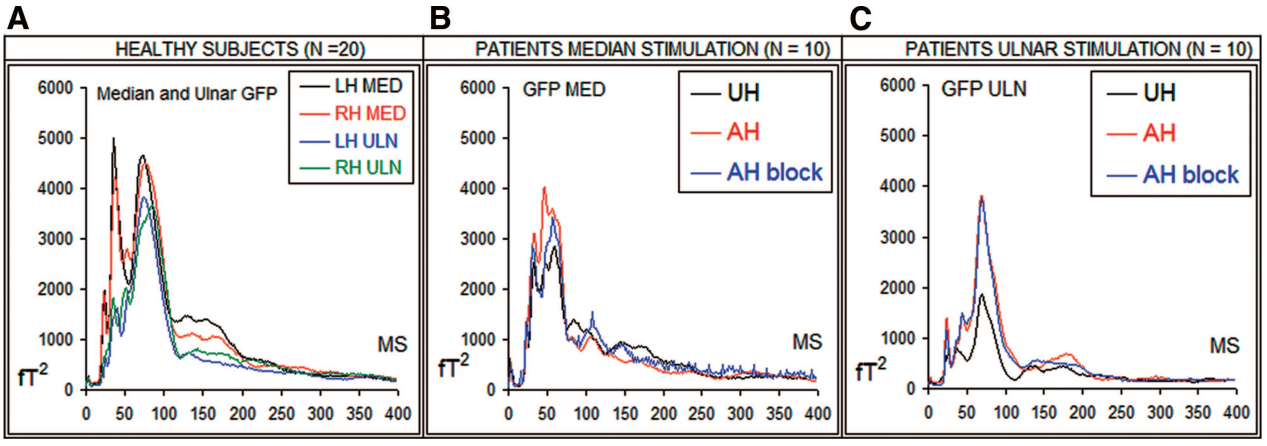

Fig. 2. The mean GFP curves of all subjects (N = 20) depict the power distribution (*A*) over the LH and RH after stimulation of the median and ulnar nerves of both hands. LH MED or LH ULN indicate the response in the LH after median or ulnar stimulation, for the RH the same meaning. *B* and *C* depict the three mean GFP curves after median and ulnar stimulation of the patient groups. The UH curve (black), the AH curve (red), and the AH after the anesthetic block (blue) are depicted. Vertical is the power in fT^2 (femtoTesla^2) and horizontal is the time in milliseconds (0–400 MS). AH = affected hemisphere; AH-block = affected hemisphere after a local block; GFP = global field power; GFP MED and GFP ULN = GFP after median and ulnar nerve stimulation, respectively; LH = left hemisphere; RH = right hemisphere; UH = unaffected hemisphere.

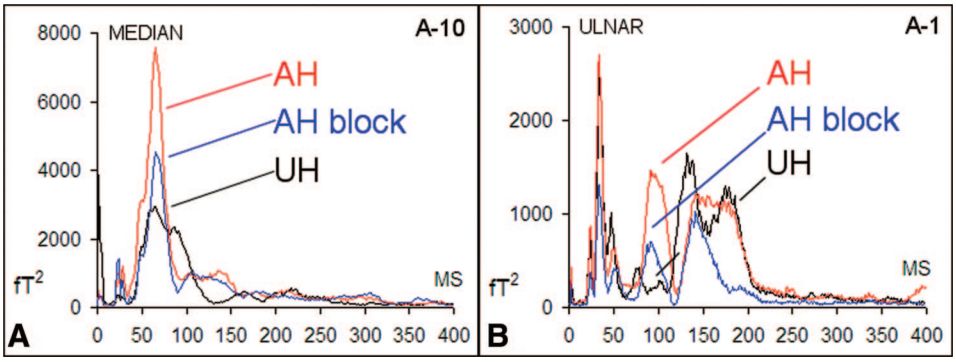

Fig. 3. Global field power (GFP) curves of patient A-10 (*A*) and patient A-1 (*B*) after median and ulnar nerve stimulation, respectively, are presented. Unaffected hemisphere (UH) (black) and affected hemisphere (AH) (red) represent the GFP curves after stimulation of the unaffected hand and affected hand; AH block (blue) depicts the GFP curve after an anesthetic block. Power differences and changes are clearly discernable after the block. Vertical is the power in fT^2 (femtoTesla^2) and horizontal is the time window in milliseconds (0–400 MS).

left hemispherical GFP response after stimulation of the right median nerve, RH med the right hemispherical GFP response after left median nerve stimulation, *etc*. Figure 2A presents the mean GFP overlay curves of the subject group after nerve stimulation. The top two curves (black and red) for the median nerve are morphologically slightly different; the same applies for the ulnar nerve (blue and green). The distribution (curves) of the power for both nerves in the entire time window is highly congruous with three distinct peaks in the first 90 ms: at M20, M30, and M70.

Patients. The morphology of the median and ulnar GFP curves (fig. 2BC, and) differed from the subject group. In the median group, the M20 and M30 peaks are part of a broad complex. In the middle stage the power in the AH is larger than in the UH, after the block the power decreases. In the ulnar group, small M20 and M30 peaks are present. At M70, AH power is larger than in the UH but after the block no difference is recognized. Strikingly in the first 90 ms poststimulus, for both the median and ulnar group,the GFP peaks in the AHs are higher, particularly between 50 ms - 90 ms compared with the UH. For subjects *versus* patients, for both patient groups the GFP peaks at M20 are hardly distinguishable but are lower compared with that of subjects. In the patient groups all the median and ulnar, M30, and M70 GFP peaks, especially in the UH, were lower compared with those of the subjects.

Patients: GFP after the Local Block (AH Block)

For the same two patients as in figure 1, the GFP curves including the effects of the anesthetic block are presented in figure 3.

The GFP curves of the responses on the AH, AH block, and UH of patient A-10 after median nerve stimulation are depicted in figure 3A. In the middle stage, around the M70 peak, clear differences are visible. After a local block with 1–2 ml lidocaine 1%, magnetoencephalography was repeated in the pain-free state. As shown, there is a considerable reduction in GFP peak value (blue) of the AH block at 68.8 ms. The individual GFP profiles in patient A-1 (fig. 3B) after ulnar stimulation differ, and power changes are observed between 30–130 ms. After the block, a considerable GFP reduction for both peaks is observed. Most consistent finding after the block for the patient group were GFP changes during the middle stage.

GFP Values at M20, M30, and M70

Based on the GFP curves of each individual subject and patient, the peak values (fT^2) were assessed. GFP data were statistically compared in and between the subject and patient groups (median and ulnar). At M20 in both groups, no statistical differences were found. In addition, no statistical differences comparing the LH and right hemisphere were found between the GFP values (in fT^2) at M30 and M70 in the subject group (table 2). The ES data, the LH as dominant hemisphere taken as control in the equation, indicate that there is hardly any difference between the right hemisphere and LH. However, no complete homology of GFP values in healthy subjects for both nerves were found.

In the middle stage, the patient groups demonstrated a significant change. At M70, after median and ulnar nerve stimulation the AH values were significantly larger compared with the UH and AH block values for both nerves (table 3). After the block in the pain-free state, no statistical difference of GFP values between the UH and the AH block was found for both nerves ($P > 0.05$). Effect size data support these findings and accentuate the effectiveness of the block.

Subjects *versus* Patients. Statistical analysis of the individual GFP data between both groups and for both hemispheres demonstrated no significant differences at M20. Table 4 presents the M30 and M70 GFP values, statistical differences, and ES data for both groups.

These data support the morphology of the GFP curves in figure 2 where in the patient groups, the M30 and M70 peaks were lower compared with those of subjects. For both patient groups, significantly lower GFP values of the UH at M30

Table 2. Mean GFP Values of Subjects

Subjects			
Median nerve mean GFP values (paired student *t* test)			
Peaks	M30 (fT^2)	Peaks	M70 (fT^2)
LH (20/20)	5,740.6	LH (20/20)	5,701.3
SD	4,954.1	SD	3,814.6
RH (20/20)	5,283.3	RH (20/20)	6,720.5
SD	3,137.7	SD	5,086.5
Diff. RH-LH*	−457.3	Diff. RH-LH*	1,019.2
ES	−0.09	ES	0.27
Ulnar nerve mean GFP values (paired *t* test)			
Peaks	M30 (fT^2)	Peaks	M70 (fT^2)
LH (18/20)	2,458.3	LH (19/20)	4,813.8
SD	2,043.3	SD	4,100.9
RH (20/20)	3,031.4	RH (20/20)	5,764.4
SD	2,969.2	SD	5,098.7
Diff. RH-LH*	573.1	Diff. RH-LH*	950.6
ES	0.28	ES	0.23

Mean GFP peak values (in femtoTesla^2 - fT^2) and SD at two latencies (M30 and M70) are presented for the subject group in both hemispheres.

ES data, numeric values, were calculated for the differences between the RH and LH. * LH is the dominant hemisphere. Numbers between brackets indicate the number of peaks in each hemisphere at M30 and M70.

ES = effect size; GFP = global field power; LH = left hemisphere; RH = right hemisphere.

and M70, in comparison to that of subjects, is demonstrated. In conclusion, significant power changes in the patient groups were found at M70 before and after the block. In contrast, between subjects and patients at M30 and M70, significant statistical power differences occur.

Three-dimensional Topography of Somatosensory-evoked Fields

Three-dimensional cortical maps were made for all subjects and patients at all major peak latencies (see Supplemental Digital Content 2, http://links.lww.com/ALN/A749, and Supplemental Digital Content and 3, http://links.lww.com/ALN/A750, presenting Median and Ulnar brain maps, respectively for two patients). In the Subject group and patient groups, the first (M20/M30) polarity reversal for both nerves was highly consistently found (more than 90–95%). The second polarity reversal in the subject group was present between M90 - M180 (more than 90%). In the patient group for all three stages and for both nerves, the second reversal differed and ranged from no to even three reversals (from M50 to M180). In the middle stage, reversals occurred several times. In the late stage (M90, M150, and M180), no second reversal between 20–80% for both nerves was present, which indicates wide variation.

Table 3. Mean GFP Values in the Patient Groups

Patients			
Median nerve mean GFP values (paired student *t* test)			
Peaks	M30 (fT^2)	Peaks	M70 (fT^2)
UH (10/10)	2,759.5	UH (9/10)	**2,826.4***
ES	0.17	ES	**1.93**
AH (9/10)	3,532.0	AH (9/10)	**5,822.3***
ES	−0.08	ES	**−0.75**
AH block (9/10)	3,180.0	AH block (9/10)	4,109.4
ES	0.09	ES	0.83
Ulnar nerve mean GFP values (wilcoxon signed rank test)			
Peaks	M30 (fT^2)	Peaks	M70 (fT^2)
UH (10/10)	555.8	UH (10/10)	**1,875.4***
ES	0.66	ES	**1.76**
AH (10/10)	880.3	AH (10/10)	**4,750.2***
ES	0.0	ES	**−0.22**
AH block (9/10)	876.0	AH block (10/10)	3,477.1
ES	0.65	ES	0.98

GFP values for the median and ulnar patient groups are presented at three stages, (UH, AH, and AH block). Numbers between brackets indicate the number of M30 and M70 peaks in each hemisphere. * A significant statistical difference was found at M70 between the UH - AH and AH - AH block values (in bold). After the block there was no significant difference between the UH - AH block values for both patient groups.

AH = affected hemisphere; AH block = affected hemisphere after the local block; ES = effect size (numeric values); GFP = global field power, values in femtoTesla^2 (fT^2); UH = unaffected hemisphere.

Table 4. Statistical GFP Comparisons between Subjects and Patients

Subjects *vs.* Patients			
Median nerve mean GFP values (student *t* test/mann-whitney ranked sum test)			
Peaks	M30 (fT^2)	Peaks	M70 (fT^2)
Mean LH + RH	5,489.5	Mean LH + RH	6,210.9
SD	4,101.0	SD	4,461.0
UH (10/10)	**2,759.5***	UH (9/10)	**2,826.4***
ES	**−0.67**	ES	**0.758**
AH (9/10)	3,532.0	AH (9/10)	5,822.3*
ES		ES	−0.087
AH block (9/10)	**3,180.0***	AH block (9/10)	4,109.4
ES	**−0.56**	ES	−0.471
Ulnar nerve mean GFP values (student *t* test/mann whitney RST)			
Peaks	M30 (fT^2)	Peaks	M70 (fT^2)
Mean LH + RH	2,737.1	Mean LH + RH	5,301.3
SD	2,517.0	SD	4,641.4
UH (10/10)	**555.8***	UH (9/10)	**1,875.4***
ES	**−0.87**	ES	**−0.70**
AH (9/10)	**880.3***	AH (9/10)	4,750.2
ES	**−0.74**	ES	−0.005
AH block (9/10)	**876.0**	AH block (9/10)	**3,477.1***
ES	**−0.74**	ES	**−0.31**

Between the subject and patients groups, at M30 and M70, GFP values were calculated. * Significant differences are presented (in bold) for both nerves. In the ES formula, the mean SD of the LH and RH was used.

AH = affected hemisphere; AH block = affected hemishere after the block; ES = effect size (values are numeric); GFP = global field power, in femtoTesla^2 (fT^2); LH = left hemisphere; RH = right hemisphere; UH = unaffected hemisphere.

ECD Characteristics

Subjects. At M20 and M30, for the median and ulnar nerve, after mirroring the dipoles to the same hemisphere, only the ulnar nerve ECD at M20 demonstrated a significantly different x-value interhemispherically. In the LH, the ulnar ECD was positioned more posterior ($P = 0.013$). The M70 ECDs in the subject groups with a low residual error (less than 6%) for both nerves present in 12–14 of 20were located in the contralateral primary somatosensory cortex. For patients, statistical analysis of M20 and M30 dipole parameters did not show any significant difference. At M70, only those ECDs with a low residual error (less than 6%) for all stages (before and after block) were studied.

Figure 4 A presents four measurements of patient A-8 after median nerve stimulation. Patient A-8 is an example of the 4 of 20 patients (see Materials) in whom a second anesthetic block was needed. The red curve depicts the GFP curve of the patient in pain. After the first block, pain was hardly present but the injured hand felt painfully cold (green curve). The GFP peaks at M30 and M70 after the first block are relatively the highest. After the second block (black curve), the AH M30 GFP peak value decreases and is comparable to the UH M30 peak (UH = 16198.2 fT^2, AH second block = 15525.7 fT^2). In the full pain-free state, the UH (blue curve) and AH-second block (black) peaks at M30 and M70 are morphologically nearly identical. In the late stage (more than 90 ms), changes are relatively low.

Figures 4B and C present a one-dimensional image of the MRI of patient A-8 with all four dipoles projected over both hemispheres at M30 and M70, respectively. The UH dipole at M30 and M70 is depicted in blue, and the AH dipoles in red. The dipole depicting the first block is green and yellow after the second block. Both at M30 and M70, the UH dipole is located more anterior, lateral, and inferior compared to all AH stages. The spatial data of the M30 and M70 dipoles in the AHs indicate that the dipoles hardly changed their positions (table 5). Combining the dipole localizations in figure 4C with the two other three-dimensional spatial images (coronal, sagittal) indicates that M70 activity is localized in the primary somatosensory cortex (see Supplemental Digital Content 4, http://links.lww.com/ALN/A751, presenting a 3-dimensional overview of the M70 dipole characteristics of patient A-8). After selection, in 6 of 10 patients (median nerve) and 5 of 10 (ulnar nerve) with a low residual error (less than 6%), the dipoles were compared with those of subjects, also located in the primary somatosensory cortex. In 9 of 20 patients M70 dipoles were not included because modeling with a single moving dipole was not possible or for reasons related to residual error (more than 6%). Combining subjects and patient data at M70, no significant statistical differences were found.

Discussion

Cortical plasticity has been defined as the central nervous system's ability to adapt to environmental challenges or compensate for lesions.[52,53] Plasticity resulted in an enhancement of cortical activity after nerve injury or amputation in humans[29–31,54] or a shrinkage of the somatosensory hand representation in complex regional pain syndrome I.[55] Be-

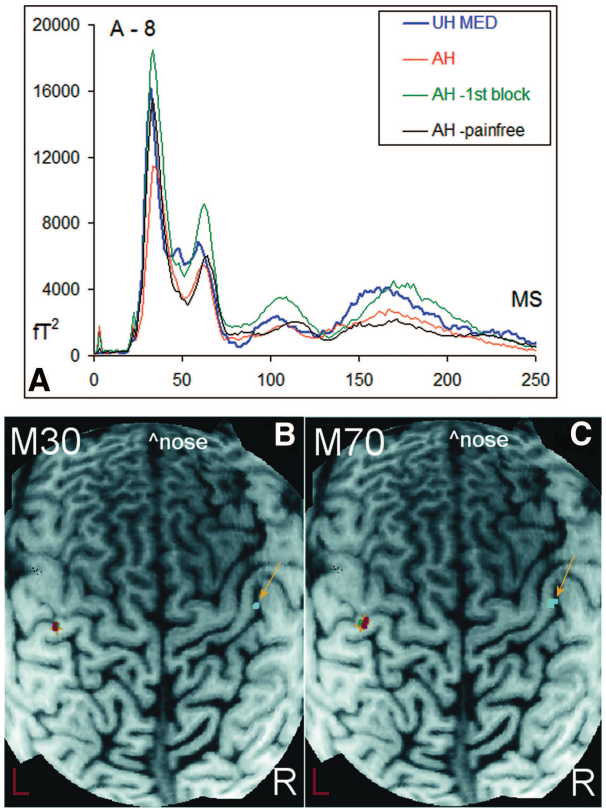

Fig. 4. (*A*) Four GFP curves of patient A-8 after four different measurements are presented. The UH curve (blue), AH in pain (red), AH first block without pain but unpleasant cold hand (green), and AH-pain free after second block without pain (black) are depicted in a 250-ms (MS) time window; vertical is the power in fT^2 (femtoTesla^2). Major power changes for patient A-8 are observed in the early (M30) and middle stage (M70). AH = affected hemisphere; AH-1st block = affected hemisphere after 1st local block; AH-pain free = affected hemisphere after 2nd local block; GFP = global field power; UH MED = unaffected hemisphere response after median nerve stimulation. The ECD localizations at M30 (*B*) and M70 (*C*) of patient A-8 are presented in the UH, AH, and AH after the first and second anesthetic block. The M30 and M70 dipoles in the UH are depicted in blue, in the AH in red. The green AH dipole depicts the dipole after the first block, minimal pain but still with an unpleasant cold hand. Yellow depicts the dipole localization after the second block. The nose is depicted in white and marks the + x axis. AH = affected hemisphere; AH-1st block = affected hemisphere after a first local block; AH pain free after second block; ECD = equivalent current dipole; L = left; M30 = ECD at 30 ms; M70 the ECD at 70 ms; R = right; UH = unaffected hemisphere.

fore the current study, stability and repeatability of the cortical evoked responses after median, ulnar, and posterior tibial nerve stimulation was assessed in subjects and PNI patients.[56,57] In this study, magnetic evoked responses in and between subjects and PNI patients were compared, before and after an anesthetic block. The GFP curves, presenting cortical activation in the subject and patient groups, differed morphologically and indicated: decreased cortical activity in the UH of both patient groups compared with the AH and AH block phase; and decreased cortical activity in patients in the AH, AH block but in particular in the UH compared with subjects. These findings are consistent with the interpretation that smaller or larger GFPs correspond to smaller or larger neural areas of activation. Therefore, our results suggest that in unilateral nerve injury of an upper extremity and continuous pain, both hemispheres are involved in cortical adaptations and hemispheric differences have to be compared with a healthy control group. The UH cannot simply serve as control to the AH. This is consistent with the observation that deafferentation in a body part elicits reorganizational changes in the sensorimotor cortex in both the contralateral and ipsilateral hemisphere.[58] Bilateral cortical reorganizational changes have been described after acute limb deafferentation[52] and in patients with nonpainful phantom limb phenomena after upper extremity amputation.[25] The mechanisms underlying these functional changes in both hemispheres were ascribed to changes in inhibitory transcallosal transmission.[52] In the patient groups, significant power changes occurred in the middle stage around M70 after the anesthetic block. In absence of the constant volley of impaired afferent information in patients with chronic neuropathic pain, central functional processes were reversible within 15 min even after years of chronic pain. At M70 after the anesthetic block and in the pain-free condition, the significant differences in GFP values between the UH and AH disappeared, a noteworthy finding. The high GFP response in patient A-8 after the first block (fig. 4A –green curve) is very interesting because it may reflect the cortical effects of sympathetic involvement in neuropathic pain.[59]

Because there were no significant stimulation threshold differences in both groups after standard electrical median and ulnar nerve stimulation at all stages of the measurements, threshold differences did not contribute to the cortical evoked magnetic responses. The CWP interindividual and intraindividual morphology differences of subjects and patients are supported by previous work.[56,60–62] CWP morphology and GFP curves indicated that the peak latencies and number of peaks of the subject and patient groups were highly consistent in the first 90 ms poststimulus period. Altered temporal processing of afferent information (facilitation) in this group of pain patients could not be demonstrated. Polarity reversals of the three-dimensional brain maps mainly reflect change in dipole orientation and are an indication of spatial somatosensory processing. The first and second polarity reversals, consistently seen in the three-dimensional maps in subjects and described earlier,[63] differed in the two groups. The significance of the finding is that in the patient group both reversals were less consistently observed and moreover at different latencies is yet unknown. It may, however, indicate altered cortical processing in the patients. These findings in patients are in agreement with experimental changes described in brain maps due to PNI in animals.[9,30,64,65]

Dipole parameters at M20 and M30 indicated that there were few differences between subjects and patients at these la-

Table 5. Median M30 and M70 Dipole Parameters

M30	Latency (ms)	Residual Error	x (mm)	y (mm)	z (mm)	Declination	Azimuth	Strength (nAm)
UH	32.0	1.4%	11.0	−45.2	72.5	118.4	208.8	52.9
AH	34.4	3.8%	2.9	36.5	82.3	93.2	172.7	52.8
AH-first block	33.6	3.3%	2.8	35.9	82.6	95.0	171.0	57.7
AH-second block	33.6	2.8%	1.8	34.5	81.7	96.5	171.1	67.0
M70		Residual error	x (mm)	y (mm)	z (mm)	Declination	Azimuth	Strength (nAm)
UH	60.4	4.2%	11.5	−42.1	73.6	118.3	212.2	36.0
AH	63.4	4.0%	4.7	32.4	85.2	106.3	153.5	34.3
AH-first block	62.4	2.9%	3.5	31.9	82.0	101.0	162.6	44.4
AH-second block	64.0	5.1%	3.4	31.7	83.3	105.2	157.3	39.9

The latencies, residual errors, and six dipole parameters of patient A-8 are presented at M30 and M70. Position values (x, y, and z) in millimeters (mm), declination and azimuth in degrees, strength in nanoAmperemeter (nAm).
AH = affected hemisphere; AH block = the hemispherical response after a first and second local anesthetic block; UH = unaffected hemisphere.

tencies. The difference between the two hemispheres at M20 for the ulnar nerve in subjects (the ulnar M20 in the LH more posterior) was not found in patients. This was in contrast with a small magnetoencephalographic study where in a group of three patients after median or ulnar transection enlarged dipole moments were found between the unaffected and affected side.[66] For all patients after median and ulnar nerve stimulation, the M70 dipoles with a low residual error (less than 6%) before and after the anesthetic block were located in the contralateral primary somatosensory cortex. The latency and position of these dipoles are in agreement with earlier studies on somatosensory processing in healthy subjects.[67–70] At M70, no bilateral hemispherical dipolar activity was found in the current study after unilateral electrical stimulation but occurred later (more than 90 ms poststimulus). This finding is in agreement with other magnetoencephalographic studies[71,72] and excludes involvement of the second somatosensory cortex.[73,74] Finally, cortical interhemispheric differences after electrical nerve stimulation were quite symmetrical in the two hemispheres, making the interhemispheric differences nondependent on age and sex.[75,76]

We conclude that in patients with neuropathic pain caused by nerve injury, major cortical changes measured by magnetoencephalography at M70 reside in the primary somatosensory cortex and may represent altered activation in the affected but also unaffected hemisphere after peripheral median and ulnar nerve stimulation. The functional cortical changes in neuropathic pain, after the modulatory effects of an anesthetic block, were found to be reversible. In these patients, an anesthetic block can valuable for the study of contralateral activation in neuropathic pain using magnetoencephalography. PNI with neuropathic pain in humans, studied with noninvasive diagnostic devices, may provide a pain model to study and monitor the effects of treatments.

Technical support was provided by Bob W. van Dijk, Ph.D., and Kees Stam, Ph.D., Professor and Head, Department of Clinical Neurophysiology and MEG Centre, VU Hospital, Amsterdam, The Netherlands. Clinical support provided by Monique A. Dekkers, M.Sc., Medical Centre Alkmaar, Alkmaar, The Netherlands.

References

1. Baron R: Peripheral neuropathic pain: From mechanisms to symptoms. Clin J Pain 2000; 16:12–20
2. Baron R: Mechanisms of disease: Neuropathic pain–a clinical perspective. Nat Clin Pract Neurol 2006; 2:95–106
3. Treede RD, Jensen TS, Campbell JN, Cruccu G, Dostrovsky JO, Griffin JW, Hansson P, Hughes R, Nurmikko T, Serra J: Neuropathic pain: Redefinition and a grading system for clinical and research purposes. Neurology 2008; 29:1630–5
4. Bridges D, Thompson SW, Rice AS: Mechanisms of neuropathic pain. Br J Anaesth 2001; 87:12–26
5. Chen R, Cohen LG, Hallett M: Nervous system reorganization following injury. Neuroscience 2002; 111:761–73
6. Woolf CJ: Dissecting out mechanisms responsible for peripheral neuropathic pain: Implications for diagnosis and therapy. Life Sci 2004; 74:2605–10
7. Costigan M, Scholz J, Woolf CJ: Neuropathic pain: A maladaptive response of the nervous system to damage. Annu Rev Neurosci 2009; 32:1–32
8. Latremoliere A, Woolf CJ: Central sensitization: A generator of pain hypersensitivity by central neural plasticity. J Pain 2009; 10:895–926
9. Dykes RW: Central consequences of peripheral nerve injuries. Ann Plast Surg 1984; 13:412–22
10. Das A: Plasticity in adult sensory cortex: A review. Network: Comput Neural Syst 1997; 8:33–76
11. Tinazzi M, Fiaschi A, Rosso T, Faccioli F, Grosslercher J, Aglioti SM: Neuroplastic changes related to pain occur at multiple levels of the human somatosensory system: A somatosensory-evoked potentials study in patients with cervical radicular pain. J Neurosci 2000; 20:9277–83
12. Malmberg A: Central changes, Pain in Peripheral Nerve Diseases, 1st edition. Edited by Reichmann H. Basel, Karger, 2001, pp 149–67
13. Stern J, Jeanmonod D, Sarnthein J: Persistent EEG overactivation in the cortical pain matrix of neurogenic pain patients. NeuroImage 2006; 31:721–31
14. Schaible HG: Peripheral and central mechanisms of pain generation. Handb Exp Pharmacol 2007; 177:3–28
15. Navarro X, Vivó M, Valero-Cabré A: Neural plasticity after peripheral nerve injury and regeneration. Prog Neurobiol 2007; 82:163–201
16. Jarvis MF, Boyce-Rustay JM: Neuropathic pain: Models and mechanisms. Curr Pharm Des 2009; 15:1711–6
17. Pons TP, Garraghty PE, Ommaya AK, Kaas JH, Taub E, Mishkin M: Massive cortical reorganization after sensory deafferentation in adult macaques. Science 1991; 252:1857–60

18. Tinazzi M, Zanette G, Volpato D, Testoni R, Bonato C, Manganotti P, Miniussi C, Fiaschi A: Neurophysiological evidence of neuroplasticity at multiple levels of the somatosensory system in patients with carpal tunnel syndrome. Brain 1998; 121:1785–94
19. Karl A, Birbaumer N, Lutzenberger W, Cohen LG, Flor H: Reorganization of motor and somatosensory cortex in upper extremity amputees with phantom limb pain. J Neurosci 2001; 21:3609–18
20. Hansson T, Brismar T: Loss of sensory discrimination after median nerve injury and activation in the primary somatosensory cortex on functional magnetic resonance imaging. J Neurosurg 2003; 99:100–5
21. Kaas JH, Collins CE: Anatomic and functional reorganization of somatosensory cortex in mature primates after peripheral nerve and spinal cord injury. Adv Neurol 2003; 93:87–95
22. Jain N, Florence SL, Qi HX, Kaas JH: Growth of new brainstem connections in adult monkeys with massive sensory loss. Proc Natl Acad Sci USA 2000; 97:5546–50
23. Borsook D, Becerra L, Fishman S, Edwards A, Jennings CL, Stojanovic M, Papinicolas L, Ramachandran VS, Gonzalez RG, Breiter H: Acute plasticity in the human somatosensory cortex following amputation. Neuroreport 1998; 9:1013–7
24. Schwenkreis P, Witscher K, Janssen F, Pleger B, Dertwinkel R, Zenz M, Malin JP, Tegenthoff M: Assessment of reorganization in the sensorimotor cortex after upper limb amputation. Clin Neurophysiol 2001; 112:627–35
25. Flor H, Mühlnickel W, Karl A, Denke C, Grüsser S, Kurth R, Taub E: A neural substrate for nonpainful phantom limb phenomena. Neuroreport 2000; 11:1407–11
26. Assmus H: Somatosensory evoked cortical potentials (SSEP) in regenerating nerves following suture. Elektroenzephalogr Elektromyogr Verwandte Geb 1978; 9:167–71
27. Tecchio F, Padua L, Aprile I, Rossini PM: Carpal tunnel syndrome modifies sensory hand cortical somatotopy: A MEG study. Hum Brain Mapp 2002; 17:28–36
28. Rossini PM, Dal Forno G: Integrated technology for evaluation of brain function and neural plasticity. Phys Med Rehabil Clin N Am 2004; 15:263–306
29. Wiech K, Preissl H, Lutzenberger W, Kiefer RT, Töpfner S, Haerle M, Schaller HE, Birbaumer N: Cortical reorganization after digit-to-hand replantation. J Neurosurg 2000; 93: 876–83
30. Florence SL, Boydston LA, Hackett TA, Lachoff HT, Strata F, Niblock MM: Sensory enrichment after peripheral nerve injury restores cortical, not thalamic, receptive field organization. Eur J Neurosci 2001; 13:1755–66
31. Stendel R, Jahnke U, Straschill M: Changes of medium-latency SEP components following peripheral nerve lesion. J Brachial Plex Peripher Nerve Inj 2006; 20:1–4
32. Ji RR, Kohno T, Moore KA, Woolf CJ: Central sensitization and LTP: Do pain and memory share similar mechanisms? Trends Neurosci 2003; 26:696–705
33. Ohara PT, Vit JP, Jasmin L: Cortical modulation of pain. Cell Mol Life Sci 2005; 62:44–52
34. Ochoa JL: Neuropathic pain: Redefinition and a grading system for clinical and research purposes (comment). Neurology 2009; 72:1282–3
35. Bruehl S, Harden RN, Galer BS, Saltz S, Bertram M, Backonja M, Gayles R, Rudin N, Bhugra MK, Stanton-Hicks M: External validation of IASP diagnostic criteria for Complex Regional Pain Syndrome and proposed research diagnostic criteria. International Association for the Study of Pain. Pain 1999; 81:147–54
36. Bruehl S: An update on the pathophysiology of complex regional pain syndrome. ANESTHESIOLOGY 2010; 113:713–25
37. Nuwer MR, Aminoff M, Desmedt J, Eisen AA, Goodin D, Matsuoka S, Mauguière F, Shibasaki H, Sutherling W, Vibert JF: IFCN recommended standards for short latency somatosensory evoked potentials. Report of an IFCN committee. International Federation of Clinical Neurophysiology. Electroencephalogr Clin Neurophysiol 1994; 91:6–11
38. Schroeder CE, Seto S, Garraghty PE: Emergence of radial nerve dominance in median nerve cortex after median nerve transection in an adult squirrel monkey. J Neurophysiol 1997; 77:522–6
39. Weiss T, Miltner WH, Huonker R, Friedel R, Schmidt I, Taub E: Rapid functional plasticity of the somatosensory cortex after finger amputation. Exp Brain Res 2000; 134:199–203
40. Weiss T, Miltner WH, Liepert J, Meissner W, Taub E: Rapid functional plasticity in the primary somatomotor cortex and perceptual changes after nerve block. Eur J Neurosci 2004; 20:3413–23
41. Tsutada T, Tsuyuguchi N, Hattori H, Shimada H, Shimogawara M, Kuramoto T, Haruta Y, Matsuoka Y, Hakuba A: Determining the appropriate stimulus intensity for studying the dipole moment in somatosensory evoked fields: A preliminary study. Clin Neurophysiol 1999; 110:2127–30
42. Olejnik S, Algina J: Measures of effect size for comparative studies: Applications, interpretations, and limitations. Contemp Educ Psychol 2000; 25:241–86
43. Nakagawa S, Cuthill IC: Effect size, confidence interval and statistical significance: A practical guide for biologists. Biol Rev Camb Philos Soc 2007; 82:591–605
44. Benjamini Y, Hochberg Y: Controlling the false discovery rate: A practical and powerful approach to multiple testing. J Roy Statist Soc Ser B (Methodological) 1995; 57:289–300
45. Perneger TV: What's wrong with Bonferroni adjustments. BMJ 1998; 18:1236–8
46. Hatem SM, Attal N, Ducreux D, Gautron M, Parker F, Plaghki L, Bouhassira D: Clinical, functional and structural determinants of central pain in syringomyelia. Brain 2010; 133: 3409–22
47. Lehmann D, Skandries W: Reference-free identification of components of checkerboard-evoked multichannel potential fields. Electroencephal Clin Neurophysiol 1980; 48:609–21
48. Skrandies W: Global field power and topographic similarity. Brain Topogr 1990; 3:137–41
49. Maurer K, Dierks Th: Data acquisition and signal analysis, Atlas of Brain Mapping, 1st edition. Edited by Maurer K, Dierks Th. Berlin, Springer-Verlag, 1991, pp 23–37
50. Vrba J, Robinson SE: Signal processing in magnetoencephalography. Methods 2001; 25:249–71
51. Fuchs M, Wagner M, Kastner J: Confidence limits of dipole source reconstruction results. Clin Neurophysiol 2004; 6:1442–51
52. Hummel F, Gerloff C, Cohen LG: Modulation of cortical function and plasticity in the human brain, Neural Plasticity in Adult Somatic Sensory-Motor Systems, 1st edition. Edited by Ebner FF. Boca Raton, Taylor & Francis Group, 2005, pp 207–27
53. Kaas JH: Functional implications of plasticity and reorganizations in the somatosensory and motor systems of developing and adult primates, The Somatosensory System. Edited by Nelson RJ. Boca Raton, CRC Press, 2001, pp 367–82
54. Elbert T, Sterr A, Flor H, Rockstroh B, Knecht S, Pantev C, Wienbruch C, Taub E: Input-increase and input-decrease types of cortical reorganization after upper extremity amputation in humans. Exp Brain Res 1997; 117:161–4
55. Maihöfner C, Handwerker HO, Neundörfer B, Birklein F: Patterns of cortical reorganization in complex regional pain syndrome. Neurology 2003; 61:1707–15
56. Theuvenet PJ, Dunajski Z, Peters MJ, van Ree JM: Responses to median and tibial nerve stimulation in patients with chronic neuropathic pain. Brain Topogr 1999; 11:305–13
57. Theuvenet PJ, van Dijk BW, Peters MJ, van Ree JM, Lopes da Silva FL, Chen AC: Whole-head MEG analysis of cortical spatial organization from unilateral stimulation of median

nerve in both hands: No complete hemispheric homology. NeuroImage 2005; 28:314–25

58. Werhahn KJ, Mortensen J, Van Boven RW, Zeuner KE, Cohen LG: Enhanced tactile spatial acuity and cortical processing during acute hand deafferentation. Nat Neurosci 2002; 5:936–8
59. Maihöfner C, Seifert F, Decol R: Activation of central sympathetic networks during innocuous and noxious somatosensory stimulation. NeuroImage 2011; 55:216–24
60. Kakigi R: Somatosensory evoked magnetic fields following median nerve stimulation. Neurosci Res 1994; 20:165–74
61. Kakigi R, Hoshiyama M, Shimojo M, Naka D, Yamasaki H, Watanabe S, Xiang J, Maeda K, Lam K, Itomi K, Nakamura A: The somatosensory evoked magnetic fields. Prog Neurobiol 2000; 61:495–523
62. Tecchio F, Pasqualetti P, Pizzella V, Romani G, Rossini PM: Morphology of somatosensory evoked fields: Inter-hemispheric similarity as a parameter for physiological and pathological neural connectivity. Neurosci Lett 2000; 287: 203–06
63. Theuvenet PJ, van Dijk BW, Peters MJ, van Ree JM, Lopes da Silva FL, Chen AC: Cortical characterization and inter-dipole distance between unilateral median *versus* ulnar nerve stimulation of both hands in MEG. Brain Topogr 2006; 19:29–42
64. Garraghty PE, Hanes DP, Florence SL, Kaas JH: Pattern of peripheral deafferentation predicts reorganizational limits in adult primate somatosensory cortex. Somatosens Mot Res 1994; 11:109–17
65. Wall JT, Xu J, Wang X: Human brain plasticity: An emerging view of the multiple substrates and mechanisms that cause cortical changes and related sensory dysfunctions after injuries of sensory inputs from the body. Brain Res Brain Res Rev 2002; 39:181–215
66. Diesch E, Preissl H, Haerle M, Schaller HE, Birbaumer N: Multiple frequency steady-state evoked magnetic field mapping of digit representation in primary somatosensory cortex. Somatosens Mot Res 2001; 18:10–8
67. Jones AK, Brown WD, Friston KJ, Qi LY, Frackowiak RS: Cortical and subcortical localization of response to pain in man using positron emission tomography. Proc R Soc Lond B Biol Sci 1991; 244:39–44
68. Hari R, Karhu J, Hämäläinen M, Knuutila J, Salonen O, Sams M, Vilkman V: Functional organization of the human first and second somatosensory cortices: A neuromagnetic study. Eur J Neurosci 1993; 5:724–34
69. Hari R, Forss N: Magnetoencephalography in the study of human somatosensory cortical processing. Philos Trans R Soc Lond B Biol Sci 1999; 354:1145–54
70. Huttunen J, Komssi S, Lauronen L: Spatial dynamics of population activities at S1 after median and ulnar nerve stimulation revisited: An MEG study. Neuroimage 2006; 32:1024–31
71. Simões C, Alary F, Forss N, Hari R: Left-hemisphere-dominant SII activation after bilateral median nerve stimulation. NeuroImage 2002; 15:686–90
72. Simões C, Hari R: Relationship between responses to contra- and ipsilateral stimuli in the human second somatosensory cortex SII. Neuroimage 1999; 10:408–16
73. Schnitzler A, Ploner M: Neurophysiology and functional neuroanatomy of pain perception. Clin Neurophysiol 2000; 17: 592–603
74. Nieuwenhuys R: The neocortex, The Human Central Nervous System, 4th edition. Edited by Nieuwenhuys R, Voogd J, Huijzen van, Chr. Berlin, Springer- Verlag, 2008, pp 683–714
75. Zappasodi F, Pasqualetti P, Tombini M, Ercolani M, Pizzella V, Rossini PM, Tecchio F: Hand cortical representation at rest and during activation: Gender and age effects in the two hemispheres. Clin Neurophysiol 2006; 117:1518–28
76. Rossini PM, Rossi S, Babiloni C, Polich J: Clinical neurophysiology of aging brain: From normal aging to neurodegeneration. Prog Neurobiol 2007; 83:375–400